Proceedings of the 11th Brazilian Congress of Thermal Sciences and Engineering -- ENCIT 2006
Braz. Soc. of Mechanical Sciences and Engineering -- ABCM, Curitiba, Brazil,- Dec. 5-8, 2006

Paper CIT06-0384

GEOMETRIC DESIGN OF CENTRIFUGAL IMPELLER BLADES USING AERODYNAMIC LOADING CRITERIA AND OPTIMIZATION TECHNIQUES

Nelson Manzanares Filho
Universidade Federal de Itajubá (UNIFEI) – Av.BPS, 1303 – CEP 37500-903 – Itajubá, MG - Brazil
nelson@unifei.edu.br

Fernando Marques Fernandes
Fundação Educacional Inaciana Padre Sabóia de Medeiros (FEI) – Av. Humberto A. Castelo Branco, 3972 – CEP 09850-901 – Sâo Bernardo do Campo, SP - Brazil
ffernandes@fei.edu.br

Waldir de Oliveira
Universidade Federal de Itajubá (UNIFEI) – Av.BPS, 1303 – CEP 37500-903 – Itajubá, MG - Brazil
waldir@unifei.edu.br

Abstract. *In this work, a low-cost computational method for blade shape design of centrifugal impellers is presented. The method is based on the use of aerodynamic loading criteria and optimization techniques. The flow model is considered two-dimensional, incompressible and irrotational and the corresponding solutions are obtained numerically by means of a straight panel method with linear vortex distributions. With the pressure an flow coefficients fixed, the shape design is carried out by means of the maximization of the local Richardson number subject to constrains over a shape factor, defined in this work. Both the maximum Richardson number and an optimum range for the shape factor are computed with the distributions of the relative velocities and pressures on the blade. A relatively narrow range was obtained for the shape factor (between 0,8 and 0,9) for pumps and fans with specific speeds between 100 and 400. In various examples, one verifies that the proposed method is able to recover the blade shape of actual centrifugal impellers of good performance and also to adequately modify the blade shape in response to required variations of the flow and pressure coefficients.Tests have shown tha the methodology is able to determine the blade shape jointly with the number of blades to be used.*

Keywords*. Turbomachinery, Centrifugal Impeller, Geometric Design of Blades, Optimization Techniques*

1. Introduction

The use of CFD techniques for turbomachinery blade design and optimization has become an irreversible trend in the last years (Kim and Park, 2000). When based on Navier-Stokes solutions, however, these techniques are very cumbersome and demand a large computational time. Moreover, the determination of some important parameters like the optimum number of blades of an impeller is still a challenge, even in the frame a powerful optimization environment. Thus, from the designer point of view, it is highly desirable to access intermediate methodologies able to define some reliable design solutions before starting a large computational task.

In the past, the use of semi-empirical formulae and diagrams, guided by the designer experience, was the main procedure for defining the preliminary turbomachine design (Baljé, 1981). Nowadays, computational methods based on potential flow solutions can be considered as an intermediate option between these rather heuristic procedures and the highly evolved CFD computations. When guided by some empirical criteria and/or boundary layer corrections, the potential flow solutions can represent the main trends of the actual flow in nominal conditions even for complex situations like that observed in centrifugal impellers (Adler and Krimerman, 1980). Further, as the potential solution can be obtained in a very small fraction of the computational time required by a corresponding Navier-Stokes solution, its use within an optimization framework is very attractive.

In this work, a low-cost computational method for blade shape design of centrifugal impellers is presented. The method is based on the use of aerodynamic loading criteria and optimization techniques. In the next section, the two-dimensional, incompressible, potential flow model used for the flow solver is presented. In section 3, the numerical solution based in the panel method is briefly described. Section 4 discusses the aerodynamic loading parameters used for guiding the optimization procedure, namely the Richardson number (Oliveira, 2001) and a shape factor for the aerodynamic load distribution (Fernandes, 2006). Section 5 succinctly describes the methodology for blade shape design, including the blade mean line parameterization, the chosen optimization algorithm and the treatment of the number of blades as a continuous design variable. In section 6, the results of two illustrative test cases are presented and discussed. The paper is concluded in section 7.

2. Potential flow formulation for centrifugal impellers of infinitely thin blades

Figure 1 shows a sketch of a centrifugal impeller with N identical and equally spaced blades, rotating clockwise at a constant angular speed ω. The blade width varies according to the function $b(r)$. The moving representative radial cascade is shown in the complex plane $z = x + iy = r\exp(i\theta)$. The absolute flow through the cascade is considered as potential ($\mathrm{rot}\,\boldsymbol{c} = 0$) and incompressible ($\mathrm{div}\,\boldsymbol{c} = 0$). The radial and circumferential velocity components of the velocity field vector $\boldsymbol{c} = c_r\mathbf{e}_r + c_\theta\mathbf{e}_\theta$ are given by $c_r(r,\theta) = \partial\Phi/\partial r$ and $c_\theta(r,\theta) = (1/r)\,\partial\Phi/\partial\theta$, respectively, where Φ represents the velocity potential function, such that $\mathrm{grad}\,\Phi = \boldsymbol{c}$. The axial velocity component is negligible and the radial width variation is accounted for by means of a two-dimensional formulation. The relative velocity is given by $\boldsymbol{w} = \boldsymbol{c} - \boldsymbol{u}$, where $\boldsymbol{u} = -\omega r\mathbf{e}_\theta$ represents the impeller tangential velocity. The normal component of relative velocity on the blade surface must be zero (impenetrability condition).

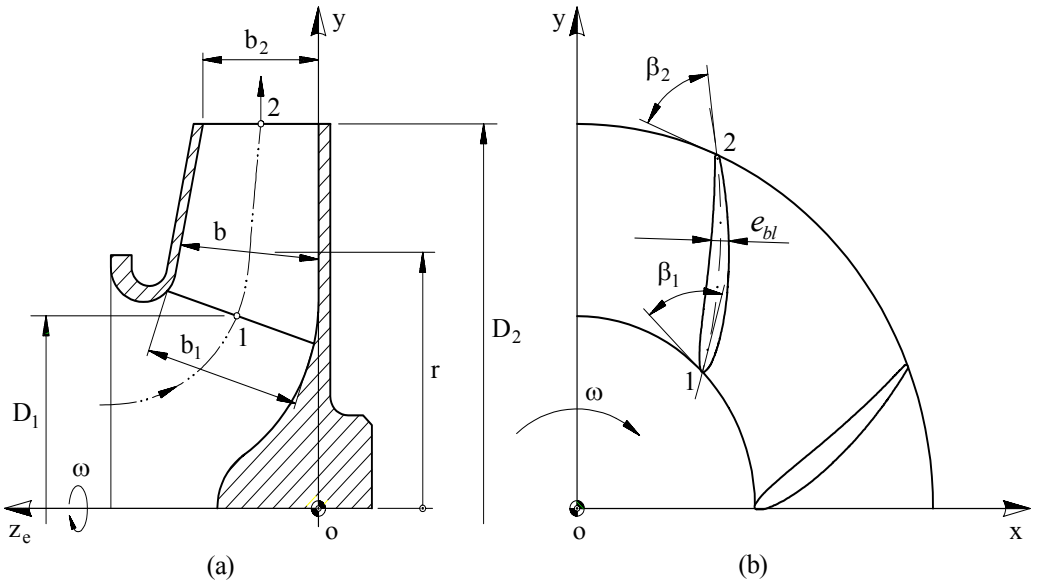

Figure 1. Sketch of a centrifugal impeller. (a) Meridian section. (b) Representative cascade.

The continuity equation (Poisson) and the impenetrability boundary condition are stated as follows:

$$\nabla^2\Phi = -\frac{1}{b(r)}\frac{db(r)}{dr}c_r(r,\theta) = B(r,\theta) \tag{1}$$

and

$$\left.\frac{\partial\Phi}{\partial n}\right|_{(\kappa)} = u_n\Big|_{(\kappa)} \tag{2}$$

where u_n is the normal component of the impeller tangential velocity on the reference blade contour (κ).

Due to the flow periodicity, the whole flow domain in the cascade plane can be divided into a series of sub-domains identical to the reference domain (D) whose contour (C) encloses the reference blade. By applying the second Green identity, it is possible to obtain the following integral formulation equivalent to Eq. (1):

$$2\pi\,\bar{c}(z) = \oint_{(C)} F(z,\zeta')\,ds' + \iint_{(D)} G(z,z')\,dA' \tag{3}$$

where

$$F(z,\zeta') = (c_n + ic_s)\,K(z,\zeta') \tag{4}$$

$$G(z,z') = B(r',\theta')\,K(z,z') \tag{5}$$

$$K(z,z') = N\,z^{N-1}\,/\,(z^N - z'^N) \tag{6}$$

and $\overline{c}(z) = (c_r - i\, c_\theta)\exp(-i\,\theta)$ is the conjugated complex velocity, c_n is the normal component pointing to the domain interior, c_s is the tangential component with the domain at left, z' and ζ' are, respectively, integration points in (D) and (C), and z is a calculation point in (D).

Considering some simplifications in the integration process (Manzanares Filho and Oliveira, 1992), Eq. (3) can be substituted by the following one (now, with the integral calculated just on the blade contour):

$$\overline{c}(z) \cong \frac{Q / b(r) - i\Gamma_o}{2\pi z} + \frac{1}{2\pi}\oint_{(\kappa)} F(z,\zeta')\, ds' \tag{7}$$

where Q and Γ_0 represent, respectively, the flow rate and the circulation at the impeller inlet.

Equation (7) is linear and accounts for perturbation singularities on the blade contour (κ) only. It differs from the classical two-dimensional case ($b(r)$ = const) just by the variable source term Q / $b(r)$.

In this work, the blades will be considered as infinitely thin, $e_{bl} \to 0$. In this case, the integral on the closed blade contour (κ) can be reduced to an open line integral between the blade leading edge, s_1, and the blade trailing edge, s_2, corresponding to points 1 and 2 of the blade mean line in Fig. (1). The normal velocity is continuous across the blade mean line and the tangential discontinuity between the suction (+) and pressure (–) sides of blade is equivalent to a vortex density, $\gamma(s') = w_s^+ - w_s^-$. It results that

$$\overline{c}(z) \cong \frac{Q / b(r) - i\Gamma_o}{2\pi z} + \frac{i}{2\pi}\int_{s_1}^{s_2} \gamma(s')\, K(z,\zeta')\, ds' \tag{8}$$

Being ζ a calculation point just on the blade mean line, the mean velocity, $\overline{c}(\zeta) = (\overline{c}(\zeta)^+ + \overline{c}(\zeta)^-)/2$, is computed by making $z = \zeta$ in Eq. (8) and interpreting the integral as a Cauchy principal value. Thus, the conjugated complex velocities in the suction and pressure sides of the blade are computed as follows:

$$\overline{c}^{\pm}(\zeta) = \overline{c}(\zeta) \mp i\,\frac{\gamma(\zeta)}{2}\, e^{-i(\theta-\beta)} \tag{9}$$

where β represents the blade angle (between the blade mean line and the circumferential direction).

The vortex density $\gamma(s)$ is determined by the impenetrability of the relative velocity across the blade mean line, Eq. (2). Using Eq. (8) and after some manipulation, this condition can be stated as follows

$$\frac{1}{2\pi}\int_{s_1}^{s_2} \gamma(s')\, L(\zeta,\zeta')\, ds' \cong \frac{Q}{2\pi\, r\, b(r)}\cos\beta - \frac{\Gamma_o}{2\pi\, r}\sin\beta - \omega\, r \sin\beta \tag{10}$$

where $L(\zeta,\zeta') = \Im m[K(\zeta,\zeta')\, e^{i(\theta-\beta)}]$ represents the normal velocity in the blade ζ point induced by a unit vortex placed at the blade ζ' point.

Equation (10) is a Fredholm integral equation of first kind for the unknown function $\gamma(s)$. Their terms represent velocity components normal to the blade mean line: the left-hand side is the contribution of the vortex distributions along the blades. At the right-hand side, the two first terms represent the contribution of a source and a vortex at origin (r = 0) and the last term is the contribution of the impeller rotation. Given ω, Q, Γ_0 and the impeller geometry, the solution of Eq. (10) is not unique. In order to obtain a unique solution, some additional condition must still be imposed. Here, we apply the classical Kutta condition, by prescribing a finite and continuous velocity at the blade trailing edge. In the present context, this can be achieved by making $\gamma(s_2) = 0$.

Knowing the vortex distribution, the absolute velocities on the blade are computed by Eqs. (8) and (9). The corresponding relative velocities are directly obtained ($\boldsymbol{w} = \boldsymbol{c} - \boldsymbol{u}$). Being w the magnitude of the relative velocity, we define a corresponding dimensionless velocity $W = w/(\omega r_2)$, where r_2 is the outlet impeller radius. We also define a dimensionless radius $R = r/r_2$ and a dimensionless pressure $P = 2(p - p_T)/(\rho\,\omega^2 r_2^2)$, where p and p_T represents the static pressure p field and the total pressure at impeller inlet, respectively. Thus, the Bernoulli theorem applied to the centrifugal impeller furnishes the following straightforward relation

$$P = R^2 - W^2 \tag{11}$$

3. Numerical solution

Equation (10) is numerically solved by means of a panel method. The blade mean line is approximated by a polygonal line of M straight segments (panels) and M+1 vertices (nodal points). A linear vortex distribution is assumed on each panel, such that the whole distribution $\gamma(s)$ becomes represented by M+1 discrete values γ_1, γ_1, …, γ_{M+1} at nodal points, with $\gamma_1 = \gamma(s_1)$ and $\gamma_{M+1} = \gamma(s_2)$. Kutta condition is directly imposed with $\gamma_{M+1} = 0$. Shockless condition at blade entrance can also be imposed similarly, by making $\gamma_1 = 0$. In this case, some flow parameter like Q or Γ_0 must result. The impenetrability condition is applied at each of the panel midpoints (control points), in such a way that Eq. (10) is approximated into a system of M linear algebraic equations with M unknowns. In general, using 40 panels is sufficient for obtaining an acceptable accuracy. After solution of the linear system, the velocity and pressure magnitudes at the control points can be easily obtained. More details about the numerical implementation can be found in Manzanares Filho (1982). About the inclusion of the impeller width variation, see Manzanares Filho and Oliveira (1992).

4. Aerodynamic loading criteria

4.1 The maximum Richardson number Ri_{max}

Baljé (1981) suggested the use of the Richardson number for adequately analyzing various flow characteristics of centrifugal impellers. Based on the considerations of Baljé (1981), Oliveira (2001) defined the local Richardson number Ri on the blade as the relation between the velocity difference across the blade, $\Delta w = w_s^+ - w_s^- = \gamma$, and the corresponding mean velocity, $\overline{w} = (w_s^+ + w_s^-)/2$:

$$\mathrm{Ri} = \frac{\Delta w}{\overline{w}} \tag{12}$$

For shockless conditions, the Richardson number is zero at the leading and trailing edges, and it attains a maximum value, Ri_{max}, somewhere along the blade. Oliveira (2001) has observed that this value can be used as an indicator of the optimum number of blades of a given shape. By varying the number of blades and computing the potential flow, it was observed that there was always a greatest value of Ri_{max} (maximum *maximorum* or max-max) for a well-defined number of blades. A number of blades different from this specific value always produced a decrease in the value of Ri_{max}. More import: by effectuating this kind of analysis for various real centrifugal impellers with geometrical and flow data reported in the literature, Oliveira (2001) verified that, as a rule of thumb, the max-max Richardson number has normally been associated with a number of blades equal or very close to the optimum number of blades reported in the literature. Thus, this max-max Richardson number could be used as a criterion for the blade number selection in centrifugal impeller design, at least for backward curved blades as that used in all of the tested impellers.

The success of the max-max Ri criterion can be explained as follows (Oliveira, 2001; Oliveira *et al.*, 2002): for a given blade shape, the value of Ri_{max} augments by increasing the aerodynamic loading, Δw, and by decreasing the mean relative velocity, $\overline{w}$. For high values of Δw, the number of blades should de low; on the other hand, for low values of $\overline{w}$, the number of blades should be high (by diminishing the shockless flow rate). Thus, the max-max Ri number acts as a compromise between situations with too low number of blades — corresponding to small friction area but with a high aerodynamic loading and a tendency for boundary layer separation — and situations with too high number of blades — corresponding to a good flow guidance inside the impeller channels but with a high friction area.

4.3 Shape design using the Richardson number

The max-max Ri criterion works well for selecting the optimum number of blades of centrifugal impellers of low specific speeds and backward curved blades of *a given fixed shape*. In this condition, however, the operating point varies with the variation of the number of blades. A question arises about the possibility of using the maximization of Ri_{max} as a criterion for the blade shape design with a *given operating point* — for instance, with fixed values for the flow rate and total pressure performed by the impeller.

For answering this question, a preliminary version of the methodology for blade shape design was implemented and tested for various impeller geometries with a given operating point. The following was observed (Fig. 2): as the number of blades was decreased from a very high one, the maximum Ri_{max} augmented without limit and occurred at positions approaching the blade trailing edge (impeller outlet). Initially, there was an expectation that, by diminishing the number of blades below a certain limit, the Ri_{max} value would eventually decrease — and so producing an optimum shape design —, but this has not occurred. At the limit, the situation of maximum Ri_{max} has leaded to impellers with a single blade, of doubtful shape, very large length and sharp curvature variations.

From these results, it was concluded that the utilization of the max-max Ri criterion exclusively was unsatisfactory for obtaining an adequate shape design for centrifugal impeller blades — where an operating point should typically be

specified. At last, it became clear the need for researching a companion loading parameter in order to better accomplish the maximization of the Richardson number and to produce feasible blade shapes.

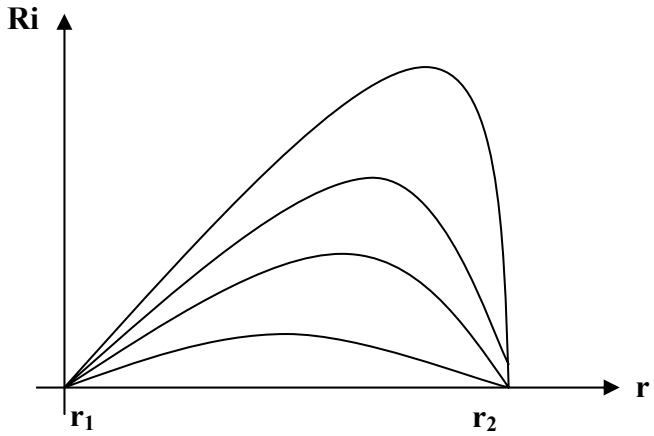

Figure 2 –Radial distribution of Richardson number for various numbers of blades and a fixed operating point. The maximum Ri increases as the number of blades decreases.

4.4 The shape factor K

It was possible to obtain another loading parameter (named here "shape factor") in order to overcome the difficulties pointed out in the previous subsection. The definition of this parameter is based on the idea that the aerodynamic loading at the rear portion of the blade should be related to the average loading along the whole blade length, as suggested by the Richardson number distributions shown in Fig. 2.

Thus, the shape factor, K, is defined as the relation between a measure of the aerodynamic loading at the rear portion of the blade, $\gamma_{max}(r_2 - r_m)$, and a measure of the average aerodynamic loading along the blade, $\gamma_{av}(r_2 - r_1)$:

$$K = \frac{\gamma_{max}(r_2 - r_m)}{\gamma_{av}(r_2 - r_1)} \tag{13}$$

where the maximum vortex density, γ_{max}, occurs at radius r_m and the average vortex density is calculated by integration over the whole blade length, $l_b = s_2 - s_1$:

$$\gamma_{av} = \frac{1}{l_b}\int_{s_1}^{s_2} \gamma \, ds \tag{14}$$

In order to illustrate the hole played by the shape factor as well as to predict a certain order of magnitude for it, let us consider a hypothetical, extremely simplified, situation of a purely radial blade ($l_b = r_2 - r_1$), with a triangular vortex distribution, as shown in Fig. 3. In this case, it is easy to verify that $\gamma_{max}/\gamma_{av} = 2$ and that Eq. (3) reduces to

$$K = 2\frac{(r_2 - r_m)}{(r_2 - r_1)} \tag{15}$$

Equation (15) indicates that the shape factor varies in the range $0 \le K \le 2$. The cases of K equal to 2, 1 and 0 are shown in Fig. 4. For K = 2 (r_m=r_1), the loading is more accentuated at the leading edge region; for K = 1 (r_m=($r_2 + r_2$)/2), the loading is more accentuated at the midpoint region; and for K = 0 (r_m=r_2), the loading is more accentuated at the trailing edge region. In cases of conventional centrifugal impellers of good performance, it is reasonable to consider that the aerodynamic loading should be well distributed along the blades instead of being more concentrated at the leading or trailing edges regions. Thus, it is expected that actual representative values for the shape factor will be closer to 1 than to 0 or 2.

For computing the shape factor in real situations by using the potential flow method described in sections 2 and 3, it is necessary to use Eqs. (13) and (14). Details about this issue can be found in Fernandes (2006).

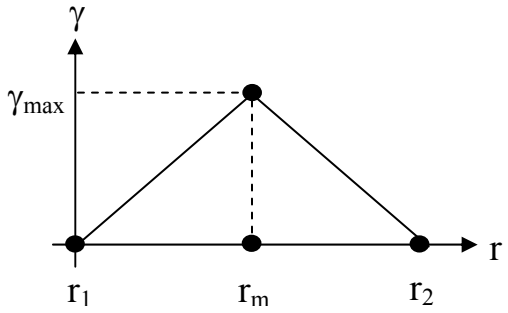

Figure 3 – Hypothetical triangular distribution for the vortex density

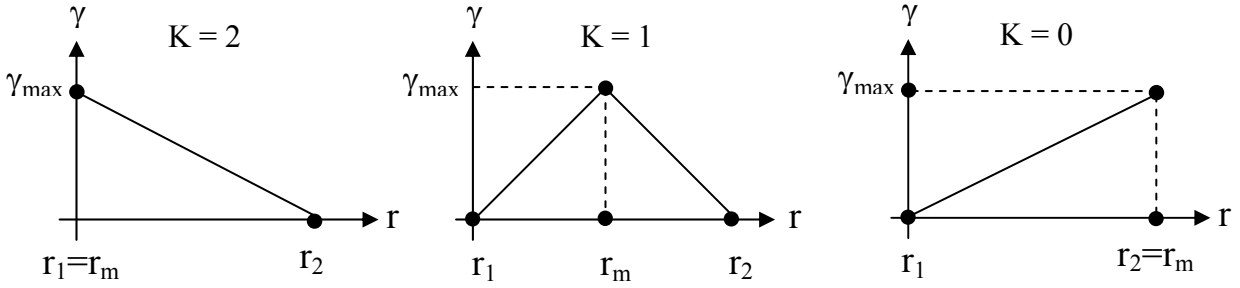

Figure 4 – Hypothetical behavior of aerodynamic loading with the shape factor variation

In order to verify the applicability of the shape factor, potential flow calculations were performed for various centrifugal impellers reported in the technical literature. Various kinds of turbomachines were considered (pumps, fans and turbocompressors), covering a wide range of specific speeds. All computations were made assuming no circulation at impeller inlet ($\Gamma_0 = 0$) and shockless entrance. Besides the loading parameters Ri_{max} and K, calculations were also made for flow coefficient, $\phi = Q/(2\pi b_2 \omega r_2^2)$, and total pressure coefficient, $\psi = 2Y/(\omega^2 r_2^2)$. Y represents the specific work performed by the impeller being proportional to the total blade circulation (Fernandes, 2006). The specific speed was also computed, $n_{qA} = 10^3\,[\omega/(2\pi)]Q^{1/2}/Y^{3/4}$.

The principal results are summarized in Table 1. For most of the tested impellers, the values obtained for the shape factor lie in a relatively narrow range, $0.8 \le K \le 0.9$, The exceptions are the impellers of Varley (1961) — whose blade shape is non-conventional — and the 7-blade impeller of Reddy and Kar (1971) — of relatively low efficiency due to an excessive number of blades, as discussed by those authors. On the other hand, the values of the maximum Richardson number lie in a significantly broader range, $0.4 \le Ri_{max} \le 1.45$.

The shadowed cells in Table 1 correspond to the optimum number of blades obtained by the max-max Ri criterion, according to Oliveira (2001). For these situations (excepting for Varley's impeller), a plot was made for the loading parameters K and Ri_{max} against specific speed, as shown in Fig. 5. It is important to note that the specific speed variation normally indicates the variation of the main geometric parameters of a turbomachine, such as diameters and widths. Usually, the nominal values of specific speed are not too much influenced by blade shape variations. Thus, it can be concluded from Fig. 5 that the maximum Richardson number is more sensitive to variations of the main geometrical parameters of impeller. This conclusion is compatible with the max-max Ri criterion, which has shown to be able to define the optimum number of fixed shape blades under varying operational conditions, but is inconclusive when an operating point is fixed. On the other hand, the optimum values of the shape factor are much less sensitive to that variation, and so can be used for better defining the blade geometry.

One can state the following: It is still possible to use the max-max Ri criterion in blade shape design of centrifugal impellers with a constrained operating point; but it is necessary in this case to guide the maximization process by also imposing constraints on the shape factor values. For this, one can impose a range for the shape factor ($0.8 \le K \le 0.9$, for instance) or define a specific value for it (for example, based on an already known design of good performance).

5. Methodology for blade shape design

In this section we describe succinctly the methodology for blade shape design of centrifugal impellers. Further details are discussed in Fernandes (2006).

Table 1 – Principal results of potential flow calculations obtained for centrifugal impellers reported in the literature.

	# Blades	b_2 mm	$D_2=2r_2$ mm	b_2/D_2	ϕ	ψ	n_{qA}	Ri_{max}	K
Kearton[1]	8	50.8	381	0.133333	0.290511	0.884891	204.68	1.06	0.85
Kearton[1]	9	50.8	381	0.133333	0.277506	0.953330	189.18	1.06	0.81
Bommes I[2]	6	78	500	0.156	0.322144	0.409533	415.49	0.43	0.84
Bommes I[2]	7	78	500	0.156	0.313125	0.469590	369.68	0.44	0.86
Bommes I[2]	8	78	500	0.156	0.306326	0.516609	340.39	0.43	0.82
Bommes II[2]	6	70	560	0.125	0.290511	0.538423	287.66	0.58	0.87
Bommes III[2]	7	50	500	0.1	0.442596	0.517395	327.21	0.55	0.83
Reddy & Kar[3]	5	7	208	0.033654	0.278296	0.769437	111.77	1.45	0.87
Reddy & Kar[3]	6	7	208	0.033654	0.260807	0.856404	99.85	1.38	0.81
Reddy & Kar[3]	7	7	208	0.033654	0.249265	0.919875	92.52	1.29	0.75
Oliveira[4]	8	32.1	419.5	0.076520	0.438215	0.922100	184.65	1.15	0.84
Oliveira[4]	10	32.1	419.5	0.076520	0.399434	1.037033	161.42	1.12	0.83
Varley[5]	5	4.5	243.84	0.018455	0.362381	0.529324	125.03	1.13	1.30
Varley[5]	6	4.5	243.84	0.018455	0.335508	0.628803	105.73	1.14	1.21

[1]Turbocompressor (Kearton, 1933); [2]Fan (Bommes, 1963); [3]Pump (Reddy and Kar, 1971); [4]Fan (Oliveira, 2001); [5]Double inlet pump, non conventional blades (Varley, 1961)

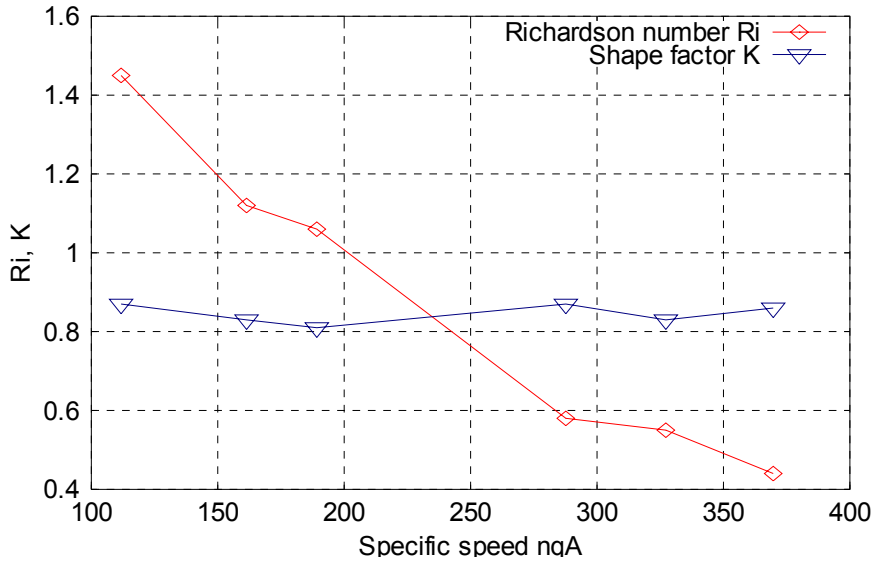

Figure 5 – Variation of aerodynamic loading parameters with specific speed

5.1 Basic problem description

In the previous section, it was concluded that a convenient approach for the blade shape design would consist in maximize the maximum Richardson number on the blade mean line (objective function) subject to constraints on the shape factor, besides of design constraints on the operating point. Thus, the basic optimization problem is stated as follows:

$$\begin{cases} \text{maximize } Ri_{max}(\mathbf{x}) \\ \text{subject to:} \quad K(\mathbf{x}) = K_0 \text{ or } K_{min} \le K(\mathbf{x}) \le K_{max} \\ \qquad\qquad \text{and constraints on } \phi \text{ and/or } \psi \text{ and/or } n_{qA} \end{cases} \tag{16}$$

A suitable algorithm is required for carrying out the optimization process (see section 5.3). The vector of design variables **x** includes the main geometrical parameters of impeller (number of blades, inlet and outlet diameters and widths) and the blade shape parameters — as described in the next subsection. It is important to note that, during the optimization process, the algorithm automatically calls for the values of Ri_{max}, ϕ, ψ and K for various impeller

geometries. These values are furnished by the potential flow solver (sections 2 and 3) with the assumptions of shockless entrance and no circulation at impeller inlet.

5.2 Parameterization of blade shape

The reference blade mean line is described by a polar curve $\theta(r)$ in the interval $r_1 \le r \le r_2$, and $\theta(r_1) = 0$. The blade mean line will be composed of a fixed basic line $\theta_b(r)$ and a perturbation line $\theta_p(r)$, such that $\theta(r) = \theta_b(r) + \theta_p(r)$, with $\theta_b(r_1) = \theta_p(r_1) = 0$. The perturbation function will be represented by a linear combination of known shape functions $f_j(r)$, $j = 0, 1, ..., M$, with $f_j(r_1) = 0$, by means of M+1 coefficients $S_0, S_1, .., S_M$:

$$\theta_P(r) = \sum_{j=0}^{M} S_j f_j(r) \tag{17}$$

where

$$f_j(r) = \left(\frac{r - r_1}{r_2 - r_1} \right)^{j+1}, \qquad j = 0, 2, \ldots \text{ (even)} \tag{18}$$

$$f_j(r) = \left[\frac{(r - r_1)(r_2 - r)}{(r_2 - r_1)^2} \right]^{j+1}, \qquad j = 1, 3, \ldots \text{ (odd)} \tag{19}$$

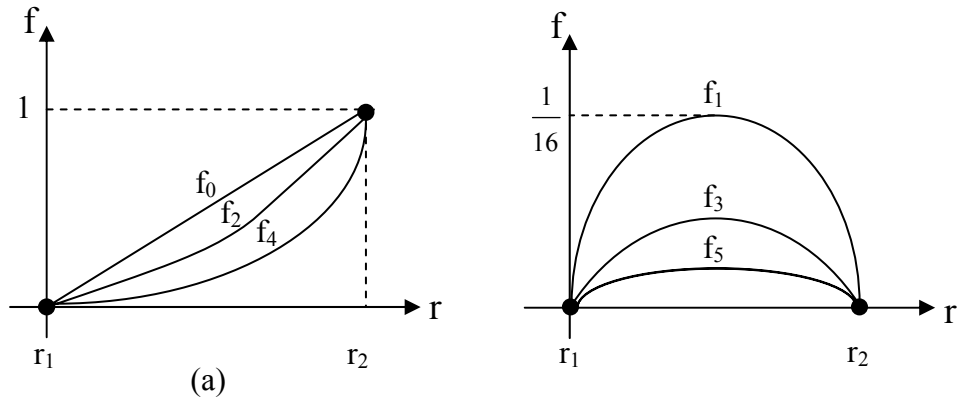

Figure 6 – Shape functions: a) of even index, b) of odd index

Some shape functions are sketched in Fig. 6. The functions of even index control mainly the perturbations of the trailing edge region relative to the leading edge; the functions of odd index control mainly the absolute perturbations along the whole blade line.

The basic line can be taken from some previous design (logarithmic or circular arc, for instance). The parameters S_j will compose the vector of design variables jointly with the main impeller dimensions and the number of blades.

5.3 Optimization algorithm

Initial tests were made using the IMSL subroutine `DNCONF` as the optimization algorithm. This routine implements a sequential quadratic programming method with equality and/or non-equality constraints. However, this routine has presented high sensibility to variations in operating conditions and shape factor. Often convergence was not attained, and we have to abandon the use of `DNCONF`.

Thence, successful tests were made using the IMSL subroutine `DUMPOL`, which has been shown to be very robust for the problem in hand. This routine is for the minimization of a continuous function of P variables by means of a direct search algorithm. The function does not need be differentiable, but general non-linear constraints are not treated by `DUMPOL`; only lateral constraints for the design variables are directly furnished to `DUMPOL`. Thus, for introducing the constraints on operating conditions and shape factor, it was necessary to apply a penalty scheme in the objective function (Ri).

The search algorithm of `DUMPOL` is based on comparisons between objective function values of a set of P+1 points in the solution space, named a *simplex* (automatically generated by `DUMPOL`, from an initial starting guess): $\mathbf{x}_1, ..., \mathbf{x}_{P+1}$. At each iteration, a new point $\mathbf{x}_k$ is generated for replacing the worst point $\mathbf{x}_j$ of the simplex (of highest objective

function value), by using the following expression: $\mathbf{x}_k = \mathbf{c} + \alpha(\mathbf{c} - \mathbf{x}_j)$, where $\mathbf{c} = (\sum \mathbf{x}_i)/\mathrm{P}$, with $i \neq j$. This corresponds to a reflection of the worst point about the centroid **c** of the remaining points of the simplex, $\alpha > 0$ being the reflection coefficient. When the new point becomes the better one, the simplex is expanded in order to avoid premature convergence. When the new point is the worst one, the simplex is contracted in order to search for a better point. A complete description of this algorithm is found in Nelder and Mead (1965).

5.4 Treating the number of blades as a continuous variable

The number of blades must be treated as a continuous design variable for using the algorithm just described. The procedure is relatively simple: it is enough to consider *N* as a real variable in Eq. 6, which is the kernel of the integral in Eq. 7. For simplifying and improving the numerical integration, one has applied a scheme similar to that employed by Petrucci *et al*. (2001) for linear cascades. It consists in summing up and subtracting the reference blade contribution, which is analytically computed as a Cauchy principal value. The remaining cascade contribution becomes naturally regularized, and can be computed by any traditional integration scheme. In this work a fast trapezoidal rule was applied and it has shown to be sufficiently accurate for impellers with a moderate number of blades (N < 20) — typical of backward bladed impellers. With this procedure, the number of blades can be treated as a continuous design variable for using routine `DUMPOL`. After determination of a non integer number of blades, the optimization code can be run again with the number of blades treated now as an integer parameter (not a variable) closer to that previously computed.

6. Results

Various tests and blade design examples were presented by Fernandes (2006). Here we present two cases using as basic geometry the fan impeller of 10 circular arc blades designed by Oliveira (2001) — see Table 1. In both tests, the inlet and outlet radius of the basic geometry were maintained and the design problem reduces just to the computation of the shape and the number of blades. The specific speed of the basic geometry was also maintained for the designed geometry. The polynomial degree M=3 was verified to be adequate and was used in both cases (Fernandes, 2006). Thus, we have five design parameters to be determined: the four S_j coefficients of the blade shape (j = 0, …,3) and the number of blades.

Case I. In the first case, the shape factor of the basic geometry was maintained (shape factor ratio, *sfr* = 1) and blade shapes were computed for 100%, 110% and 90% of the original total pressure coefficient (pressure coefficient ratio, *pcr* = 1, 1.1 and 0.9, respectively). The results for the main design characteristics, the resulting blade shapes and the corresponding pressure distributions on the blade are presented in Table 2 and Figs. 7 and 8. First, we note that in this case the flow coefficient must vary as $(pcr)^{3/2}$ in order to maintain the specific speed. Some small numerical errors were observed for satisfying the constraints when *pcr* = 1. Even with all working parameters fixed, a design shape was obtained that corresponds to a number of blades different of the original design (first line of Table 1). In comparison with this situation, the variation of the pressure coefficient leads to an expected trend: an increase (decrease) in pressure and flow coefficients produces a greater (smaller) number of blades (Table 1) and shorter (longer) blades with greater (smaller) blade angles along the whole blade line (Fig. 7). This was expected since a more (less) opened channel produces more (less) angular momentum and more (less) flow rate. In Fig. 8, we observe that the pressure distributions along the blades follow a coherent trend: more (less) total pressure performed by the impeller corresponds to blades more (less) aerodynamically loaded. It is also observed a greater influence of the total pressure variation on the blade suction side as compared with the pressure side. This issue may be restrictive in the case of pump impellers due to cavitation limit requirements. Further, note that the maximum Richardson number follows the same trend as the aerodynamic loading, as it would be expected in this case (Table 1).

Case II. In the second case, the total pressure coefficient of the basic geometry was maintained (*pcr* = 1) and blade shapes were computed for 100%, 110% and 90% of the original shape factor (*sfr* = 1, 1.1 and 0.9, respectively) The results for the main design characteristics, the resulting blade shapes and the corresponding pressure distributions on the blade are presented in Table 3 and Figs. 9 and 10. Note that the variation of shape factor has much less influence on the blade shape than total pressure variation (compare Figs. 9 and 7). This was expected since the impeller operating point is fixed is this case, and blade shape variations are also related to the variation in the number of blades. Observe that the increase in the shape factor produces an impeller with a greater number of blades and less aerodynamic loading. On the other hand, a decrease in the shape factor is much less influential both in terms of blade shape and in terms of aerodynamic loading. Note that the shape factor was intentionally varied a little outside its recommended range, $0{,}8 \leq K \leq 0{,}9$ (see Table 1). Thus, a still smaller effect is expected if the shape factor is maintained within that range, which is desirable in the context of the design methodology proposed in this work.

Some further remarks: In all the cases, the number of function evaluations required for convergence of the optimization algorithm can be considered reasonable (Tables 2 and 3). The non integer numbers of blades obtained in the examples should not cause confusion: once obtained such a solution, it is enough to run again the computational code with a closer integer number of blades fixed (as already explained in section 5.4). So the methodology produces not only the blade shape but also an estimation of the number of blades to be used, within an integrated frame.

Table 2 – Main impeller characteristics for Case I (*sfr* = 1)

pcr	**# Blades (original)**	**# Blades (computed)**	**Ri_{max}**	**K**	**ϕ**	**Ψ**	**# Function evaluations**
1.0	10	8.99	1.2341	0.8318	0.3994	1.0370	500
1.1	10	10.44	1.2474	0.8320	0.4608	1.1407	463
0.9	10	8.64	1.0338	0.8320	0.3410	0.9333	616

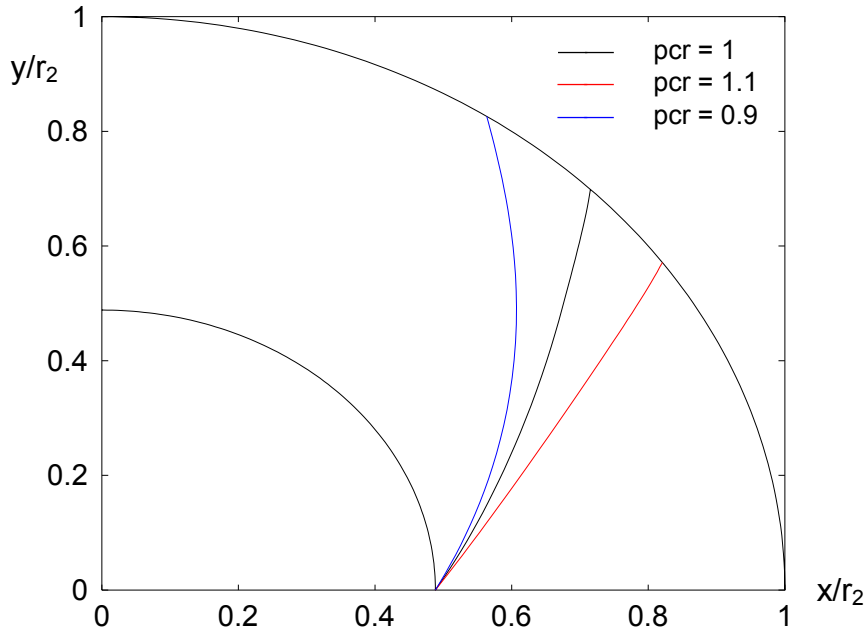

Figure 7 – Blade shapes obtained for the Case I (*sfr* = 1)

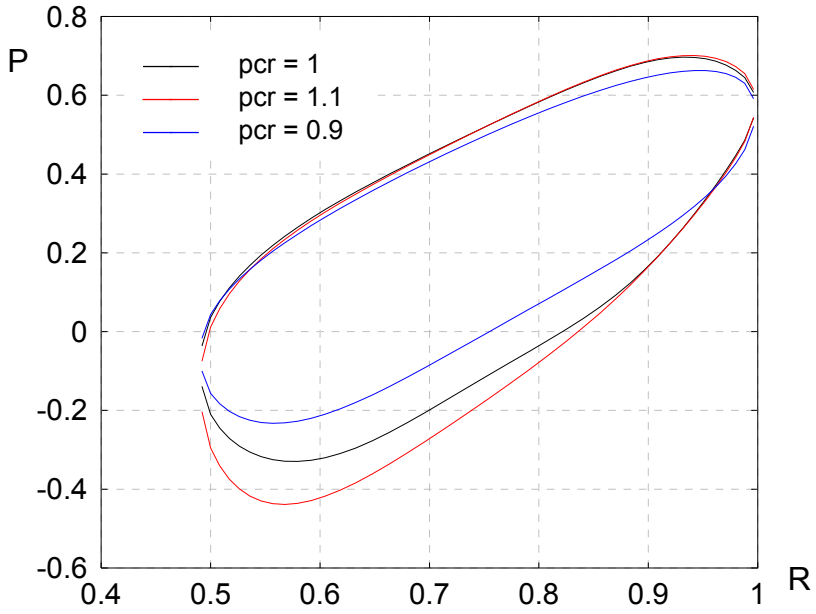

Figure 8 – Pressure distributions obtained for the Case I (*sfr* = 1)

Table 3 – Main impeller characteristics for Case II (*pcr* = 1)

sfr	**# Blades (original)**	**# Blades (computed)**	**Ri_{max}**	**K**	**ϕ**	**Ψ**	**# Function evaluations**
1.0	10	8.99	1.2341	0.8318	0.3994	1.0370	500
1.1	10	11.56	1.0469	0.9150	0.3994	1.0370	724
0.9	10	8.88	1.1612	0.7486	0.3994	1.0370	417

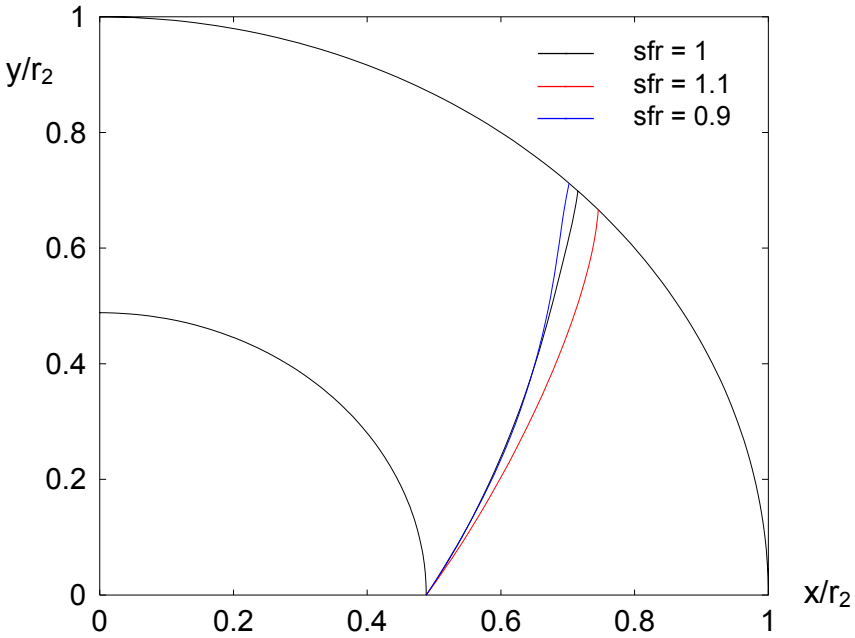

Figure 9 – Blade shapes obtained for the Case II (*pcr* = 1)

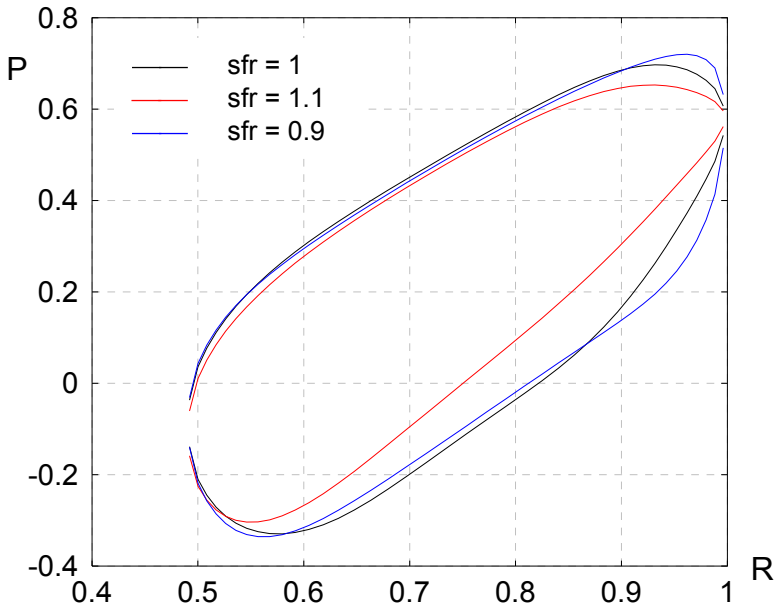

Figure 10 – Pressure distributions obtained for the Case II (*pcr* = 1)

7. Conclusion

The methodology presented is this work has shown to be able to recover the blade shape of actual centrifugal impellers of good performance and also to adequately modify the blade shape in response to required variations of the working conditions. The optimum shape and number of blades are simultaneously computed, each one influencing the other.

The methodology has a low computational cost since it is based on a potential flow solver. The neglecting of the viscous effects, however, has been circumvented by a judicious combination of the max-max Ri criterion and a narrow range for the shape factor K — which has been proposed and validated in this work. The shape factor range defines a suitable distribution for the aerodynamic loading along the blade and controls mainly the shape of the blade; on the other hand, the max-max Ri criterion controls mainly the number of blades of the impeller, as already shown in previous works.

In a design framework, the proposed methodology can be used for preliminary tests of several geometrical options before one has to engage in a larger amount of computational endeavor, using evolved CFD solvers. Thus, the more complex computational tasks would be performed mainly for the sake of refinement, diminishing in this way the overall time taken for completing the whole design program.

8. References

Adler, D. and Krimerman, Y., 1980, "On the relevance of inviscid subsonic flow calculations to real centrifugal impellers flows", ASME Journal of Fluids Engineering, Vol. 102, pp. 78-84.

Baljé, O. E., 1981, "Turbomachines - A Guide to Design, Selection, and Theory", John Wiley & Sons, Inc..

Bommes, L., 1963, "On the influence of the Number of Blades on the Basic Line for Centrifugal Fans with Backward Curved Blades (in German)", Heizung - Lüftung - Haustechnik, Nr. 5, S. 206-209.

Fernandes, F. M., 2006, "Geometric Design of Centrifugal Impeller Blades Using Aerodynamic Loading Criteria and Optimization Techniques (in Portuguese)", MSc Dissertation, Universidade Federal de Itajubá, Itajubá, MG, Brazil.

Kearton, W. J., 1933, "The Influence of the Number of Impeller Blades on the Pressure Generated in a Centrifugal Compressor and on its General Performance", Proceedings of the Institution of Mechanical Engineers, Vol. 124, pp. 481-568.

Kim, J. S. and Park, W. G., 2000, "Optimized Inverse Design Method for Pump Impeller", Mechanics Research Communication, Vol. 27, No 4, pp. 465-473.

Manzanares Filho, N., 1982, "Potential Flow in Radial Cascades of Turbomachinery (in Portuguese)", MSc Dissertation, Universidade Federal de Itajubá, Itajubá, MG, Brazil.

Manzanares Filho, N and Oliveira, W., 1992, " Potential Flow Calculation for Centrifugal Impellers with Thin Blades and Variable Width (in Portuguese)", Proceedings of ENCIT 1992, the 4th Brazilian Congress of Thermal Sciences and Engineering, ABCM, Rio de Janeiro, RJ Brazil, pp. 297-300.

Nelder, J.A., and Mead, R., 1965, "A Simplex Method for Function Minimization", Computer Journal, Vol. 7, pp 308-313.

Oliveira, W., 2001, "Flow Analysis in Radial Turbomachinery (in Portuguese)", Doctoral Thesis, Instituto Tecnológico de Aeronáutica, S. J. dos Campos, SP, Brazil.

Oliveira, W., Manzanares Filho, N. and Fernandes, E. C., 2002, " A Criterion Based on Local Flow Characteristics for Determinations of the Optimum Number of Blades of Turbomachinery Impellers (in Portuguese)", Proceedings of ENCIT 2002, the 9th Brazilian Congress of Thermal Sciences and Engineering , ABCM, Caxambu , MG, Brazil, Paper CIT02-0440.

Petrucci, D. R., Manzanares Filho, N. and Camacho, R. G. R., 2001, "An Efficient Panel Method Based on Linear Vortex Distributions for Flow Analysis in Turbomachinery Cascades (in Portuguese)", Proceedings of COBEM 2001, 16th Brazilian Congress of Mechanical Engineering, ABCM, Uberlândia, MG, Brazil, Vol. 8, pp. 256-265.

Reddy, Y. R. and Kar, S., 1971, "Optimum Vane Number and Angle of Centrifugal Pumps with Logarithmic Vanes", ASME Journal of Basic Engineering, Vol. 93, pp. 411-425.

Varley, F. A., 1961, "Effects of Impeller Design and Surface Roughness on the Performance of Centrifugal Pumps", Proceedings of the Institutional Mechanical Engineers, Vol. 175, No. 21, pp. 955-989.

9. Copyright Notice